TPAC V1 Paper

J. A. Ballin*, J. P. Crooks†, P. D. Dauncey*, A.-M. Magnan*, Y. Mikami‡, O. D. Miller‡, M. Noy*, V. Rajovic‡, M. M. Stanitzki†, K. D. Stefanov†, R. Turchetta†, M. Tyndel†, E. G. Villani†, N. Watson‡, J. A. Wilson‡

July 15, 2008

Abstract

ECAL, CMOS blah.

*Department of Physics, Blackett Laboratory, Imperial College London, London.
†STFC, Rutherford Appleton Laboratory, Chilton, Didcot.
‡School of Physics and Astronomy, University of Birmingham, Birmingham.

Contents

1 Introduction - ~ 2 pages

Context of the ILC. ECAL important for hadronic jet resolution for PFA. Sampling binary RCAL.

ILC operation will consist of bunch trains, a short burst of O(1000) bunch crossings lasting O(msec), followed by a quiet period of O(sec). Data are buffered on sensor during the bunch train and read out following this during the quiet period.

2 Requirements - ~ 5 pages

2.1 Electromagnetic shower properties

MIPs better measure of shower energy than deposited energy. Density of MIPs in 500 GeV showers.

2.2 ILC requirements

Pixel size. Timing. Hit rate and noise. Machine background.

2.3 Others

Power.

3 Design - ~ 10 pages

3.1 Overall architecture

Top-level overview.

Figure 1: Sensor overall architecture.

3.2 Fabrication and INMAPS

0.18 μm CMOS INMAPS process.

3.3 Pre-shaper pixel

Circuit, parameters.

Figure 2: Pre-shaper pixel circuit.

Mode of operation.

3.4 Pre-sampler pixel

Circuit, parameters.

Mode of operation.

Figure 3: Pre-sampler pixel circuit.

3.5 Mask and trim configuration

Operation. Load method. Readback.

3.6 Data storage

Memory operation. Dead area. Memory limit.

3.7 Readout

Operation of readout columns. Speed limitation.

3.8 Known design issues

Details of three bugs. Crosstalk and power.

3.9 DAQ system and operation

USB_DAQ and support PCB. Bonding and yield issues. Operating parameters for all following measurements are 400 ns bunch crossings. Grounding of substrate.

4 Single pixel performance - ~ 10 pages

4.1 Circuit simulation

Expected noise, gain.

Figure 4: Simulation of noise.

4.2 Charge spread simulation

Charge spread. Signal size vs. position. Overall efficiency for MIP vs. threshold.

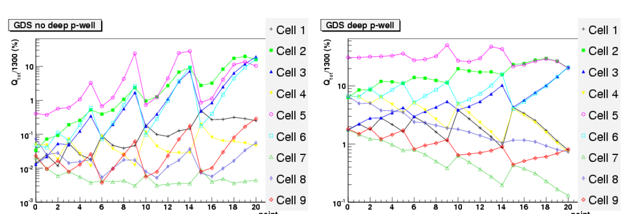

Figure 5: Simulation of charge spread for (left) no deep p-well and (right) deep p-well

Overall efficiency for MIP vs. threshold.

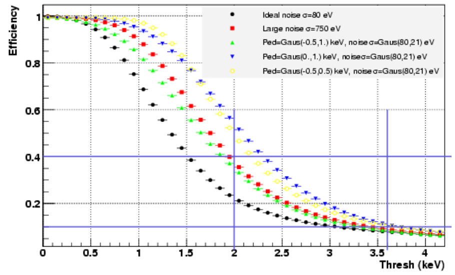

Figure 6: Simulation of efficiency vs. threshold.

4.3 Test pixel performance

Analogue noise,

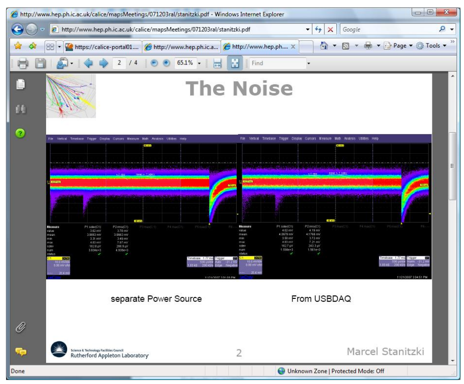

Figure 7: Test pixel noise.

gain (from laser),

Figure 8: Test pixel laser signal.

calibration of pre-samplers gain (from ^{55}Fe);

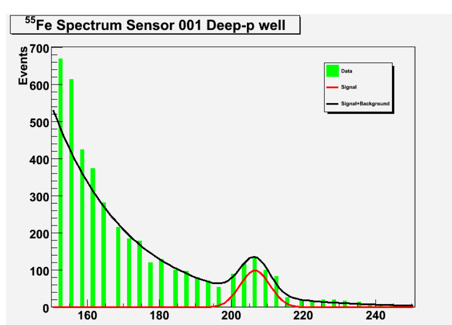

Figure 9: Test pixel ^{55}Fe signal.

compared to simulation.

Laser charge spread vs. position; compared to simulation with and without deep p-well.

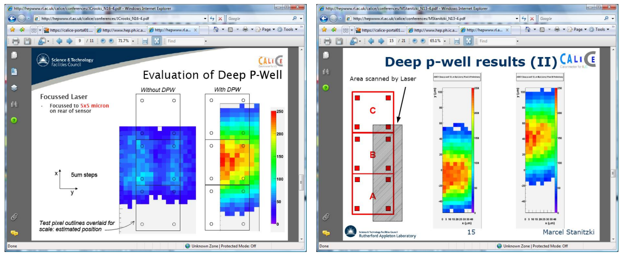

Figure 10: Test pixel charge spread.

4.4 Bulk pedestal and noise

Analogue pedestal and noise from threshold scan.

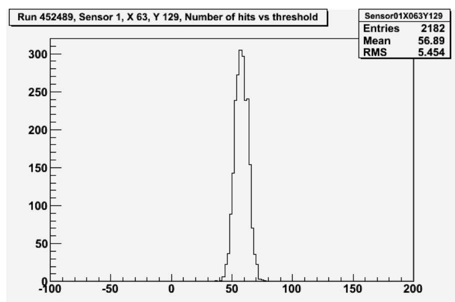

Figure 11: Typical channel threshold scan.

Pedestal and noise distributions for quadrants 0 and 1.

Figure 12: Distributions of (left) pedestals and (right) noise for quadrant 0 (solid histogram) and 1 (dashed histogram).

Uniformity vs. position.

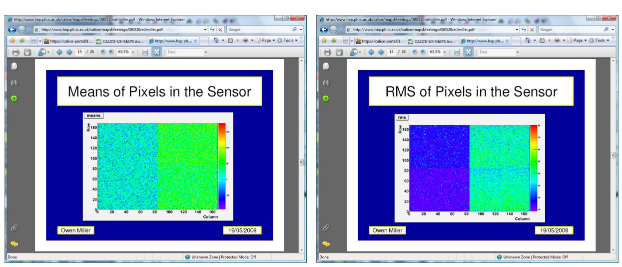

Figure 13: Two-D map of (left) pedestals and (right) noise for a typical sensor.

Effect of trim

Effect of resets at start of bunch train. Effect of substrate ground.

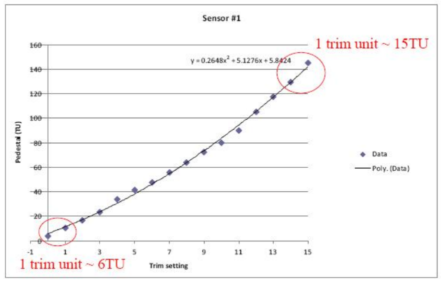

Figure 14: Typical channel trim scan.

4.5 Bulk laser signal response

Measurement of laser signal.

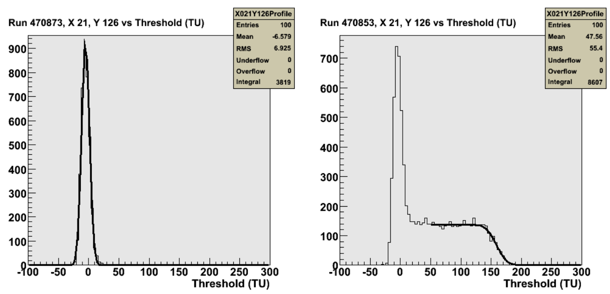

Figure 15: Threshold scan (left) without and (right) with laser.

Effect of focus and hence substrate tilt.

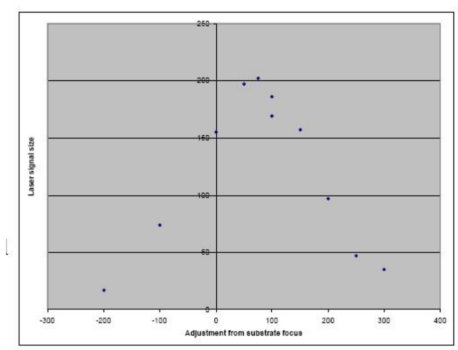

Figure 16: Signal size vs laser focus.

Optimisation of S/N with biases.
Gain (from laser),
calibration of bulk pre-samplers and pre-shapers; compared to simulation.
Laser charge spread vs. position; compared to simulation with and without deep p-well.

Figure 17: Laser signal/noise as a function of various bias DAC settings.

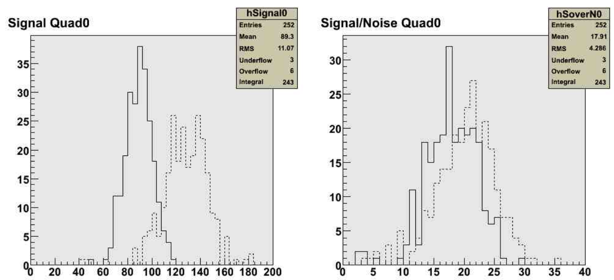

Figure 18: Laser (left) signal and (right) signal/noise for quadrants 0 (solid line) and 1 (dashed line).

Figure 19: Two-D map of laser gain for typical sensor.

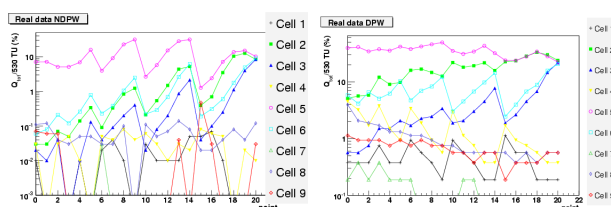

Figure 20: Charge seen at each impact point for each pixel (right) without deep p-well and (left) with deep p-well.

5 Sensor performance - ~ 10 pages

5.1 Configuration load

Error rates from sensor load.

5.2 Noise and crosstalk

Crosstalk;

dependence on masking, position.

Single pixel plots in 4 done with only pixel studied unmasked.

Possible cause of crosstalk, how to fix.

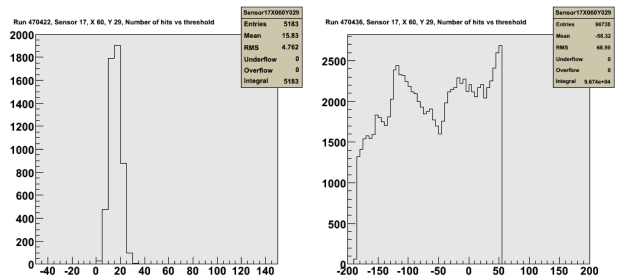

Figure 21: Effect of crosstalk on typical pixel (left) single pixel enabled (right) all pixels enabled.

Figure 22: Onset of crosstalk as number of unmasked channels increases.

5.3 Hit corruption

Twinning, corruption rates using hitOverride.

5.4 Source response

Efficiency vs threshold for ^{90}Sr.

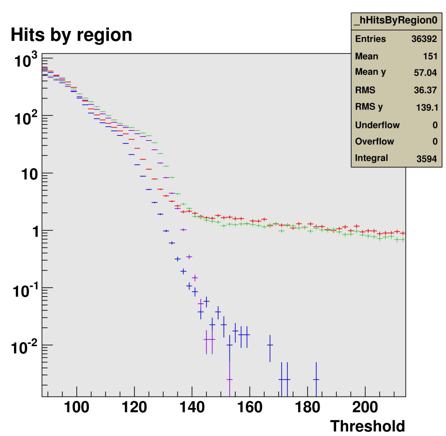

Figure 23: Rate of hits vs threshold for ^{90}Sr.

Calibration peak for ^{55}Fe).

Figure 24: Rate of hits vs threshold for ^{55}Fe.

5.5 Beam test

DESY, Dec 2007 for one week. Around 100 runs, XXX TBytes. Explain ran with no trim, crosstalk, high threshold.

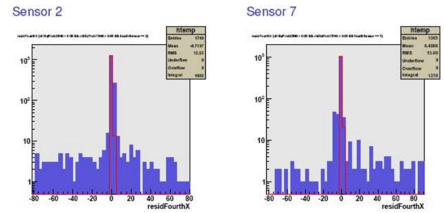

Figure 25: Residuals on inner sensors.

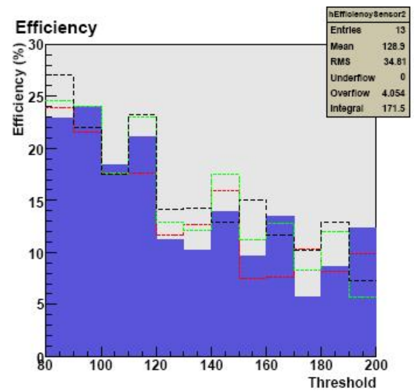

Figure 26: Efficiency vs threshold.

As a tracker; residuals.

Measure pedestal separately, correct to "real" threshold. Relative efficiency vs real threshold, comparing real threshold distribution for all and for hit pixels.

Figure 27: Distribution of real thresholds for all and hit pixels.

Figure 28: Relative efficiency vs real threshold.

5.6 Cosmics

Absolute MIPS efficiency

Figure 29: Efficiency vs real threshold.

6 Physics performance - ~ 5 pages

6.1 Simulation

GEANT4 and Mokka. Verified using general CALICE beam test.

6.2 MIP counting

Weighting of neighbours.

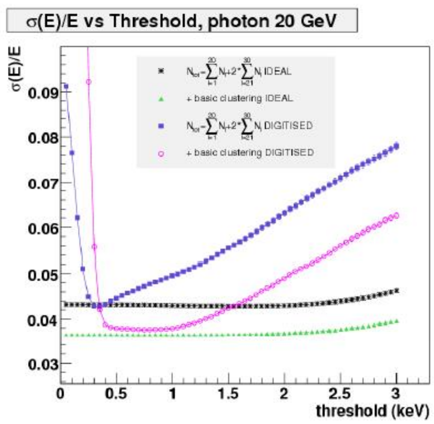

Figure 30: Effect of MIP counting.

6.3 Electromagnetic shower resolution

Resolution with and without INMAPS deep p-well.

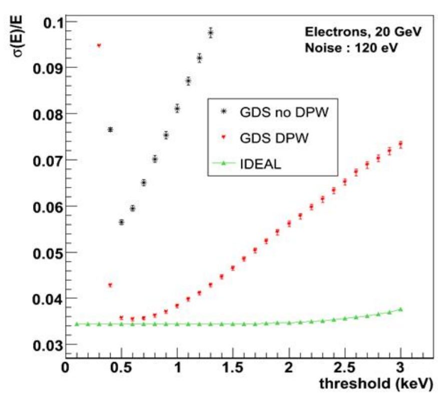

Figure 31: Resolution with and without deep p-well including MIP counting.

6.4 Hadronic jet resolution

No-harm case.

Improvements.

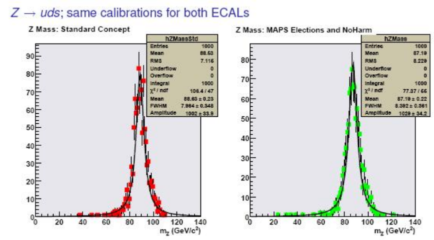

Figure 32: Hadronic jet resolution for “no-harm” case.

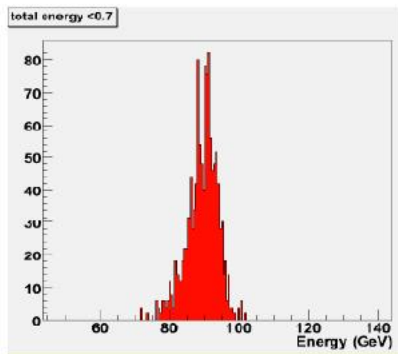

Figure 33: Hadronic jet resolution with PFA-improved algorithm.

7 Conclusions - ~ 2 pages

Proven INMAPS deep p-well. Proven pixel design adequate. Proven DECAL will work better than AECAL.

Need work on overall sensor crosstalk and trims/pedestal variations.